KSME

Springer

Journal of Mechanical Science and Technology 34 (10) 2020

Original Article
DOI 10.1007/s12206-020-2203-z

Keywords:
· Condition-based maintenance
· Hotelling's T^2 chart
· Nonparametric control chart
· One class support vector machine
· Prognostics and health management

Correspondence to:
Suk Joo Bae
sjbae@hanyang.ac.kr

Citation:
Mun, B. M., Lim, M., Bae, S. J. (2020). Condition monitoring scheme via one-class support vector machine and multivariate control charts. Journal of Mechanical Science and Technology 34 (10) (2020) 3937~3944.
http://doi.org/10.1007/s12206-020-2203-z

Received April 27th, 2020
Revised May 12th, 2020
Accepted May 12th, 2020

† This paper was presented at ICMR-2019, Maison Glad Jeju, Jeju, Korea, November 27-29, 2019.
Recommended by Guest Editor Insu Jeon

Condition monitoring scheme via one-class support vector machine and multivariate control charts

Byeong Min Mun, Munwon Lim and Suk Joo Bae

Department of Industrial Engineering, Hanyang University, Seoul, Korea

Abstract A condition-based maintenance (CBM) has been widely employed to reduce maintenance cost by predicting the health status of many complex systems in prognostics and health management (PHM) framework. Recently, multivariate control charts used in statistical process control (SPC) have been actively introduced as monitoring technology. In this paper, we propose a condition monitoring scheme to monitor the health status of the system of interest. In our condition monitoring scheme, we first define reference data set using one-class support vector machine (OC-SVM) to construct the control limit of multivariate control charts in phase I. Then, parametric control chart or non-parametric control chart is selected according to the results from multivariate normality tests. The proposed condition monitoring scheme is applied to sensor data of two anemometers to evaluate the performance of fault detection power.

1. Introduction

Prognostics and health management (PHM) has been widely used to monitor the health status of the operating system. Its future health status can be efficiently predicted using advance sensing technology and artificial intelligence (AI) for the purpose of fault isolation or reliability prediction [1]. PHM methodology targets to provide prognostic information or knowledge on the monitoring system to prevent catastrophic failures of the system by predicting the time to failure or estimating remaining useful life during operation, resulting in significantly reducing total operational cost. In applying PHM concept to maintenance, a condition-based maintenance (CBM) has an increasing attention in many complex systems (e.g., power plants, large transportation vehicles) as a predictive maintenance approach. CBM activities have been conducted based on the prediction of remaining useful life until a failure occurs, thus it can greatly reduce maintenance cost caused by unnecessary preventive maintenance tasks [2].

In many practical applications, univariate or multivariate control charts have been widely used as a process monitoring technique in statistical process control (SPC) areas. Among them, the most popular control chart is a Hotelling's T^2 chart for monitoring multivariate process variables under a parametric framework [3]. Besides, multivariate exponential weighted moving average (EWMA) charts [4] or cumulative sum (CUSUM) charts [5] have been used to efficiently detect gradual changes in the process. The above charts are constructed under the assumption that the data follows a multivariate normal distribution to control Type I and Type II errors [6]. To overcome the limitation of the multivariate normal assumption, various nonparametric control charts have been proposed. For example, Hayter and Tsui [7] proposed a Shewhart-type nonparametric multivariate control chart based on the M statistic. Sun and Tsung [8] introduced the multivariate control chart based on the kernel distance called the *K*-chart. Bae et al. [9] proposed a nonparametric multivariate control chart based on data depth such as Mahalanobis depth and Tukey depth. Based on data mining and machine learning methods, Sukchotrat et al. [10] proposed nonparametric control charts which apply the effectiveness of one-class classification to phase i and phase II analysis. He et al. [11] suggested a distance-based control chart for monitoring multivariate processes using support vector machines

(SVMs). However, the application of control chart to CBM is not easily observed in the reliability literature.

Rasay et al. [12] introduced the application of multivariate control charts as the condition monitoring technique. Recently, Bae et al. [13] proposed the condition monitoring of a steam turbine generator using the Hotelling's T^2 chart based on wavelet spectrum analysis. In this paper, we propose a condition monitoring scheme via one-class support vector machine (OC-SVM) and multivariate control charts. The condition monitoring scheme aims to derive an appropriate decision boundary of the in-control state using OC-SVM. In multivariate control charts, statistics are determined by reference data defined as the in-control state. In order to apply the reference data set defined by OC-SVM to multivariate control charts, the multivariate normality test is conducted for multivariate normal checking purpose. Once the multivariate normality is satisfied, Hotelling's T^2 chart can be employed, otherwise, a multivariate nonparametric chart can be used.

The rest of this paper is organized as follows. In Sec. 2, we illustrate the OC-SVM to determine reference data set under the in-control state. In Sec. 3, we discuss both the parametric and the nonparametric control charts: The Hotelling's T^2 chart and data depth based nonparametric control chart. In Sec. 4, we propose a condition monitoring scheme via OC-SVM and multivariate control charts. In Sec. 5, we apply the proposed methods to sensor measure data collected from the anemometers. Finally, we conclude in Sec. 6 with a discussion on future research.

2. One-class support vector machine

SVM is one of the most efficient supervised learning algorithms originated in statistical learning theory [14]. The SVM is a linear model that constructs nonlinear class boundaries by mapping input vectors into a high-dimensional feature space. Because the linear model in the new space represents nonlinear class boundaries in the original space, it does not involve any computational cost in the high-dimensional space [15]. In many practical applications, the SVM has been widely applied to classification, regression, and novelty detection problems.

Dealing with novelty detection or one-class classification, an OC-SVM constructs a spherical decision boundary by using support vectors describing the sphere boundary [16]. Tax and Duin [17, 18] proposed a support vector domain description (SVDD) algorithm by combining SVM and the data description method to solve the one-class classification problem. Schölkopf et al. [19] suggested an alternative approach to solve the one-class classification problem, where the primal optimization problem for the OC-SVM is defined as

$$\begin{aligned} &\text{Minimize} && \frac{1}{2}\|\mathbf{w}\|^2+\frac{1}{m\nu}\sum_{i=1}^{m}\xi_i-\rho \\ &\text{Subject to} && \left(\mathbf{w}\cdot\mathbf{\Phi}(\mathbf{x}_i)\right)\geq\rho-\xi_i, \\ & && \xi_i\geq 0,\ \ i=1,\ldots,m, \end{aligned} \tag{1}$$

Table 1. Kernel function for one-class SVM.

Kernel	Equation
Gaussian RBF kernel	$\exp\left(-\sigma\|\mathbf{x}-\mathbf{x}'\|^2\right)$
Laplace RBF kernel	$\exp\left(-\sigma\|\mathbf{x}-\mathbf{x}'\|\right)$
Polynomial kernel	$\left(\text{scale}\langle\mathbf{x},\mathbf{x}'\rangle+\text{offset}\right)^{\text{degree}}$

where m is the number of observations, $\mathbf{w}$ are the solutions of OC-SVM, ξ_i's are non-zero slack variables, and ν is an upper bound on the fraction of outliers. The primal optimization problem can be solved by using a Lagrangian multiplier:

$$\begin{aligned} L(w,\xi,\rho,\alpha_i,\beta_i)=&\frac{1}{2}\|w\|^2+\frac{1}{m\nu}\sum_{i=1}^{m}\xi_i-\rho \\ &-\sum_{i=1}^{m}\alpha_i\left(\left(\mathbf{w}\cdot\mathbf{\Phi}(\mathbf{x}_i)\right)-\rho+\xi_i\right) \\ &-\sum_{i=1}^{m}\beta_i\xi_i, \end{aligned} \tag{2}$$

where $\alpha_i\,(\geq 0)$ and $\beta_i\,(\geq 0)$ are Lagrangian multipliers. By setting the partial derivatives of Eq. (2) with respect to the primal variables $\mathbf{w}, \xi_i, \rho$, and equal to zero, we obtain

$$\begin{aligned} &\mathbf{w}=\sum_{i=1}^{m}\alpha_i\mathbf{\Phi}(\mathbf{x}_i), \\ &\alpha_i=\frac{1}{m\nu}-\beta_i,\ \ i=1,\ldots,m, \\ &\sum_{i=1}^{m}\alpha_i=1. \end{aligned} \tag{3}$$

The Lagrangian multiplier Eq. (2) by using the constraints Eq. (3) can be rewritten as the following dual quadratic programming problem:

$$\begin{aligned} &\text{Minimize} && \sum_{i,j=1}^{m}\alpha_i\alpha_j k(\mathbf{x}_i,\mathbf{x}_j) \\ &\text{Subject to} && 0\leq\alpha_i\leq\frac{1}{m\nu},\ \ i=1,\ldots,m, \\ & && \sum_{i=1}^{m}\alpha_i=1. \end{aligned} \tag{4}$$

Because Eq. (4) is a typical quadratic problem, it can easily be solved in a standard quadratic programming solver.

The OC-SVM replaces the inner product $\langle\mathbf{\Phi}(\mathbf{x}),\mathbf{\Phi}(\mathbf{x}')\rangle$ with the kernel function $k(\cdot)$ that performs nonlinear mapping in high-dimensional feature space. This is often referred to as the kernel trick represented by a kernel function [16]

$$k(\mathbf{x},\mathbf{x}')=\left(\mathbf{\Phi}(\mathbf{x})\cdot\mathbf{\Phi}(\mathbf{x}')\right). \tag{5}$$

By using the kernel function, OC-SVM constructs the spherical decision boundary by mapping input vectors into a high-dimensional feature space. The widely used kernel functions include the Gaussian radial basis function (RBF) kernel, the Laplace radial basis function (RBF) kernel, and polynomial

kernel, which are summarized in Table 1.

3. Multivariate control chart

A multivariate control chart is one of the widely used SPC techniques for quality control. The most popular multivariate control chart is Hotelling's T^2 chart proposed by Hotelling [3]. Suppose that the reference observation $\mathbf{z}$ has a p dimensional multivariate normal distribution with mean vector $\boldsymbol{\mu}$ and variance-covariance matrix Σ. The T_i^2 statistic of the Hotelling's T^2 chart for individual observations is defined as

$$T_i^2 = (\mathbf{z}_i - \boldsymbol{\mu})^T \boldsymbol{\Sigma}^{-1} (\mathbf{z}_i - \boldsymbol{\mu}), \quad i = 1, \ldots, m. \tag{6}$$

If the mean vector $\boldsymbol{\mu}$ and variance-covariance matrix Σ are unknown, the T_i^2 statistic is given by

$$T_i^2 = (\mathbf{z}_i - \overline{\mathbf{z}})^T \mathbf{S}^{-1} (\mathbf{z}_i - \overline{\mathbf{z}}), \quad i = 1, \ldots, m, \tag{7}$$

where $\overline{\mathbf{z}}$ is a sample mean vector and $\mathbf{S}$ is a sample variance-covariance matrix determined from the reference data. The sample vector $\mathbf{z}$ follows a multivariate normal distribution. The Hotelling's T^2 chart uses the reference data to construct upper control limit (UCL) to designate an in-control state in phase I. The UCL of the Hotelling's T^2 chart in phase II is determined by

$$UCL = \frac{p(m-1)^2}{m(m-p)} F_{\alpha, p, n-p,} \tag{8}$$

where m is the number of observations, p is the number of variables, and $F_{\alpha,p,n-p}$ is the upper αth quantile of the F distribution with the first degrees of freedom p and the second degrees of freedom $n-p$. The UCL Eq. (8) can be used to monitor the health status of the system in our condition monitoring scheme. If the test statistic Eq. (7) falls above the UCL, the system is declared as out-of-control. The Hotelling's T^2 control chart works well under the multivariate normal distribution. However, most multivariate data from complex systems may fail to follow multivariate normal distribution [20]. To address this limitation, many nonparametric control charts have been proposed [7-9].

To define faulty status of the system, we introduce a nonparametric control chart proposed by Liu [21], called r chart, in this work. This chart uses the concept of data depth to reduce each of multivariate measurements to a univariate measure. Suppose that there are reference observations $\{\mathbf{z}_1, \ldots, \mathbf{z}_\mathrm{m}\}$ from a distribution G and new observations $\{\mathbf{y}_1, \mathbf{y}_2, \ldots\}$ from a distribution F. The r chart is Shewhart-type chart for individual measurements based on data depth function. From G-distributed reference observations $\{\mathbf{z}_1, \ldots, \mathbf{z}_\mathrm{m}\}$, $\mathrm{r_G}$ statistic is given by

$$\mathrm{r_G}(\mathbf{y}) = \mathrm{P}\{\mathrm{D_G}(\mathbf{z}) \le \mathrm{D_G}(\mathbf{y}) | \mathbf{z} \sim \mathrm{G}\},$$

where $\mathrm{D_G}(\cdot)$ is a data depth function. If the distribution of $\mathrm{D_G}(\cdot)$ is unknown, $\mathrm{r_{G_m}}$ statistic is defined as

$$\mathrm{r_{G_m}}(\mathbf{y}) = \frac{\#\{\mathbf{z}_\mathrm{j} \mid \mathrm{D_{G_m}}(\mathbf{z}_\mathrm{j}) \le \mathrm{D_{G_m}}(\mathbf{y})\}}{\mathrm{m}}, \quad \mathrm{j} = 1, \ldots, \mathrm{m}. \tag{9}$$

The $\mathrm{r_{G_m}}$ statistic Eq. (9) indicates how close a new observation is to the center of the reference observation. If the $\mathrm{r_{G_m}}$ statistic Eq. (9) falls below lower control limit (LCL) α, the system is declared as out-of-control.

In order to construct r chart, we use Mahalanobis depth and Tukey depth. Tukey [22] introduced a data depth concept to characterize the high-dimensional data. Zuo and Serfling [23] established a general statistical definition of depth function that satisfies four properties: Affine invariance, maximality at center, monotonicity relative to deepest point, and vanishing at infinity. The Mahalanobis depth [24] is given by

$$\mathrm{MD_G}(\mathbf{z}) = \frac{1}{1 + (\mathbf{z} - \boldsymbol{\mu})^\mathrm{T} \Sigma^{-1} (\mathbf{z} - \boldsymbol{\mu})},$$

with mean vector $\boldsymbol{\mu}$ and variance-covariance matrix Σ. The Mahalanobis depth is based on Hotelling's T^2 statistic Eq. (6). It indicates how close the reference observation is with respect to the distribution G. In general, because G is unknown, the Mahalanobis depth is calculated as

$$\mathrm{MD_{G_m}}(\mathbf{z}_\mathrm{i}) = \frac{1}{1 + (\mathbf{z}_\mathrm{i} - \overline{\mathbf{z}})^\mathrm{T} \mathbf{S}^{-1} (\mathbf{z}_\mathrm{i} - \overline{\mathbf{z}})},$$

with a sample mean vector $\overline{\mathbf{z}}$ and a sample covariance-variance matrix $\mathbf{S}$.

Taking all possible one-dimensional projections into account, Tukey depth [22] is known as a half-space depth which is the smallest proportion of data points. The Tukey depth for reference data with respect to the distribution G is given by

$$\mathrm{TD_G}(\mathbf{z}) = \inf_\mathrm{H}\{\mathrm{P_G}(\mathrm{H})\},$$

where H is a closed half space. If the distribution G is unknown, the Tukey depth is calculated as

$$TD_{G_m}(\mathbf{z}) = \frac{1}{m} \min_i \{\min(k_i, n - k_i)\},$$

where $k_i = \psi_1(i) - \psi_2(i)$ for $\psi_1(i) = \#\{j : 0 \le \theta_j < \theta_i + \pi\}$ and $\psi_2(i) = \#\{j : 0 \le \theta_j < \theta_i\}$, θ_i is the angle of $u_i = (\mathbf{z}_i - \mathbf{z}) / \|\mathbf{z}_i - \mathbf{z}\|$. See Bae et al. [9] for more details on the properties of the data depths.

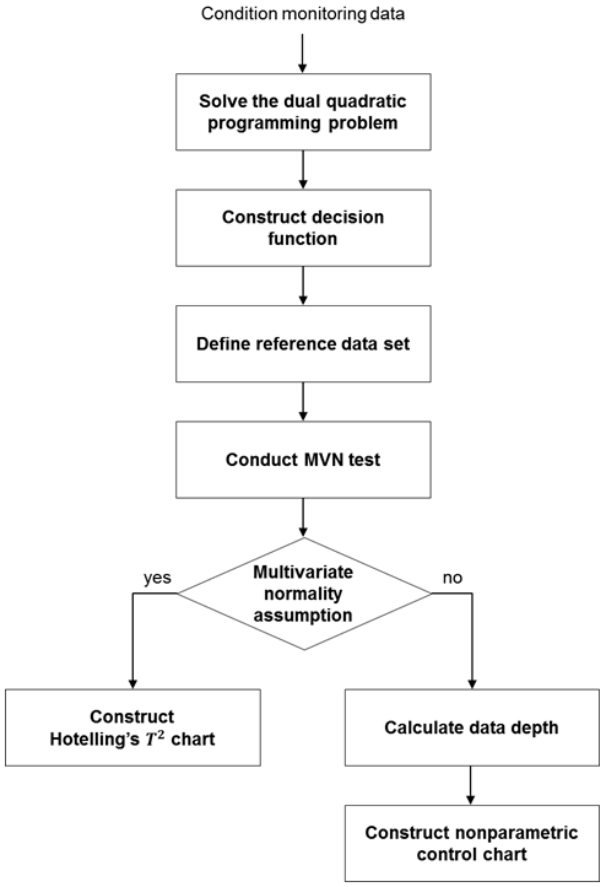

Fig. 1. The proposed condition monitoring scheme via OC-SVM and multivariate control charts.

4. Condition monitoring scheme

In this section, we propose a condition monitoring scheme via OC-SVM and multivariate control charts. The detailed procedure of suggested monitoring scheme is given in Fig. 1. To derive an appropriate decision boundary of the in-control state of the system, OC-SVM is employed. In the proposed monitoring scheme, the multivariate normality test is conducted to apply parametric control charts like Hotelling's T^2 chart. If the normality assumption is not satisfied, nonparametric charts using the concept of data depths is applied.

General control limits of the multivariate control charts are determined by reference data set in an in-control state. Alt [25] and Jackson [26] discussed how to construct the control limits. However, it is still practically hard to decide the standard for the in-control state. We suggest a decision function of the OC-SVM to define the reference data set in the in-control state. In the primal optimization problem Eq. (1) for the OC-SVM, the decision function of OC-SVM can be obtained from the following equation:

$$f(\mathbf{x}) = \operatorname{sgn}\left(\left(\mathbf{w}\cdot\mathbf{\Phi}(\mathbf{x})\right) - \rho\right). \tag{10}$$

By using the kernel function Eq. (5), the decision function Eq. (10) can be rewritten as the following equation:

$$f(\mathbf{x}) = \operatorname{sgn}\left(\sum_i \alpha_i k(\mathbf{x}_i, \mathbf{x}_j) - \rho\right). \tag{11}$$

The Lagrange multiplier α_i can be solved by the quadratic programming problem Eq. (4). If the decision function Eq. (11) is positive, data set $\mathbf{x}_j$ exists in spherical decision boundary. On the other hand, if the decision function is negative, data set $\mathbf{x}_j$ will be located outside of the spherical decision boundary and considered as faulty status. The reference data set in in-control state by using the decision function is defined as

$$\mathbf{z} = \left\{\mathbf{x}_j \,\middle|\, \sum_i \alpha_i k(\mathbf{x}_i, \mathbf{x}_j) - \rho > 0\right\}.$$

Next, we introduce two widely used multivariate normality test statistics to check the normality of the reference data set $\mathbf{z}$. Based on multivariate skewness and kurtosis measures, the multivariate normal (MVN) test statistics [27] are

$$\hat{\gamma}_1 = \frac{1}{m^2}\sum_{i=1}^{m}\sum_{j=1}^{m} M_{ij}^3 \sim \chi^2_{p(p+1)(p+2)/6},$$

and

$$\hat{\gamma}_2 = \frac{1}{m}\sum_{i=1}^{m} M_{ij}^2 \sim N\left(p(p+2), 8p(p+2)/m\right),$$

respectively, where p is the number of variables and M_{ij} is the squared Mahalanobis distance, which is defined as $M_{ij} = (\mathbf{z}_i - \bar{\mathbf{z}})^T \boldsymbol{S}^{-1}(\mathbf{z}_j - \bar{\mathbf{z}})$. Based on the distance between two distribution functions, Henze and Zirkler [28] suggested the following the test statistics

$$HZ = \frac{1}{m}\sum_{i=1}^{m}\sum_{j=1}^{m}\exp\left(-\frac{\beta^2}{2}D_{ij}\right) - 2\left(1+\beta^2\right)^{-\frac{p}{2}} \times\sum_{i=1}^{m}\exp\left(-\frac{\beta^2}{2\left(1+\beta^2\right)}D_i\right) + m\left(1+2\beta^2\right)^{-\frac{p}{2}} \sim LN\left(\mu, \sigma^2\right),$$

where $\beta = 1/\sqrt{2}\left[m(2p+1)/4\right]^{1/(p+4)}$, $D_{ij} = (\mathbf{z}_i - \mathbf{z}_j)^T \boldsymbol{S}^{-1}(\mathbf{z}_i - \mathbf{z}_j)$, and $D_i = (\mathbf{z}_i - \bar{\mathbf{z}})^T \boldsymbol{S}^{-1}(\mathbf{z}_i - \bar{\mathbf{z}})$. D_{ij} is the Mahalanobis distance between ith and jth observations and D_i is the squared Mahalanobis distance of ith observation to the centroid. Using the two normality test statistics, we select an appropriate control chart between parametric and nonparametric control charts.

5. Application

The proposed condition monitoring scheme is applied to time

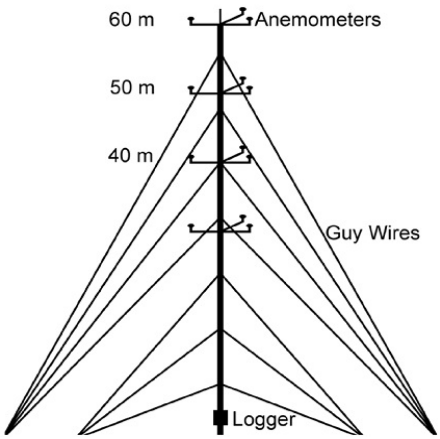

Fig. 2. Example of the anemometers of the meteorological tower (https://www.windpowerengineering.com).

series data of two anemometers. A three-cup anemometer (shown in Fig. 2) is the device used to measure wind speeds. We used the data set which is given in https://www.phmsociety.org/competition/phm/11/problem. Wind speed sensor data are collected from two anemometers at the same height. The data was repeatedly recorded in five-day intervals over one year and the measurements from sensors consist of the summary statistics such as mean, maximum value, and minimum value in every ten minutes from each sensor. The details on the used anemometers and the characteristics of the data are given in the website. Several researchers proposed the condition monitoring methods to detect faulty status of anemometers. For example, Sun et al. [29] introduced a condition monitoring procedure of data preprocessing, feature extraction, and pattern identification, for the condition diagnosis of an anemometer. Because the two sensors at the equal height measure the wind speed, the measured data must be almost the same. Thus, we calculated the difference between two measured values to detect anomaly status of the sensor.

Figs. 3(a) and (b) present the mean values of the measurements over every ten minutes from sensor 1 and sensor 2, respectively. The difference between two values are also given in Fig. 3(c). We have only partial information about failure-times; that is, the number of intervals including abnormal conditions of the anemometers is equal to 17 among 73 intervals, but we don't have any information about exact time points of the abnormal conditions. Thus, it is challenging to classify the normal and abnormal conditions of the anemometer sensors.

First, we applied OC-SVM to define reference data set which is assumed to stand for the normal condition of the anemometers. The performance of OC-SVM depends highly on the selected kernel function and its hyperparameter values. This study employed two kernel functions: The RBF kernel and the polynomial kernel. For example, the performance of the OC-SVM with RBF kernel depends the hyperparameter σ and ν. The hyperparameter of OC-SVM, ν, which is the upper bound on the fraction of outliers, controls the complexity of spherical decision boundary for the OC-SVM. The best combi-

Table 2. Grid-search results using the RBF kernel in OC-SVM.

ν	σ					
	2^{-5}	2^{-3}	2^{-1}	2^{1}	2^{3}	2^{5}
0.91	67	67	67	67	67	67
0.93	67	67	67	67	67	67
0.95	67	67	67	67	67	67
0.97	67	66	66	66	66	67
0.99	64	64	64	65	65	65

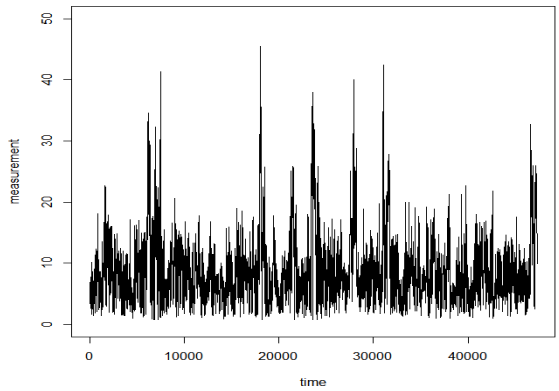

(a) Mean values from sensor 1

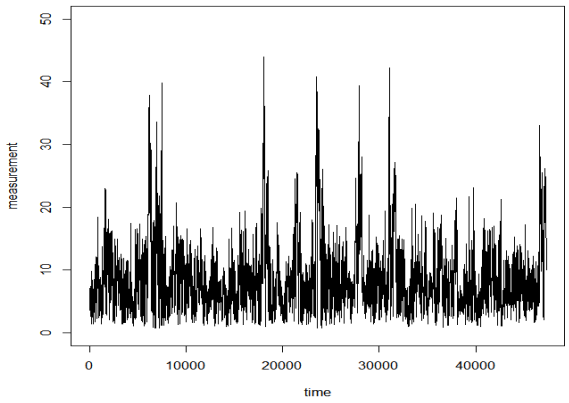

(b) Mean values from sensor 2

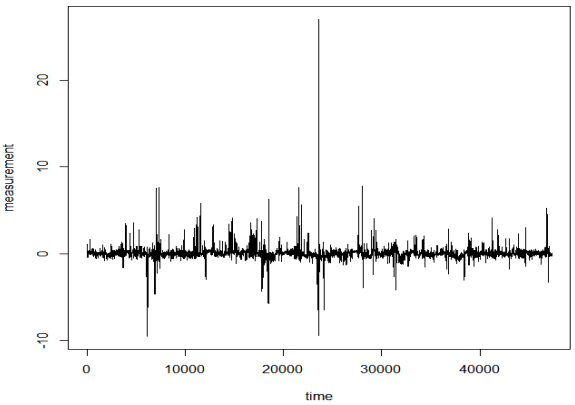

(c) Difference of measurements between sensors 1 and 2

Fig. 3. Mean values of the measurements over every ten minutes.

Table 3. Grid-search results using the polynomial kernel in OC-SVM.

D	ν	σ					
		2^{-5}	2^{-3}	2^{-1}	2^{1}	2^{3}	2^{5}
2	0.91	67	67	67	67	67	67
	0.93	67	67	67	67	67	67
	0.95	62	62	62	62	62	62
	0.97	43	43	43	43	43	43
	0.99	21	21	21	21	21	21
3	0.91	10	18	20	20	20	20
	0.93	9	19	19	19	19	19
	0.95	7	15	**17**	**17**	**17**	**17**
	0.97	6	13	20	20	20	20
	0.99	8	12	11	11	11	11
4	0.91	67	67	67	67	67	67
	0.93	67	67	67	67	67	67
	0.95	62	62	62	62	62	62
	0.97	42	42	42	42	42	42
	0.99	20	20	20	20	20	20

Table 4. Multivariate normality (MVN) test.

Test		Statistic	p-value
Mardia's MVN test	Skewness	12050.6979	< 0.0001
	Kurtosis	242.6030	< 0.0001
Henze-Zirkler's MVN test		87.0672	< 0.0001

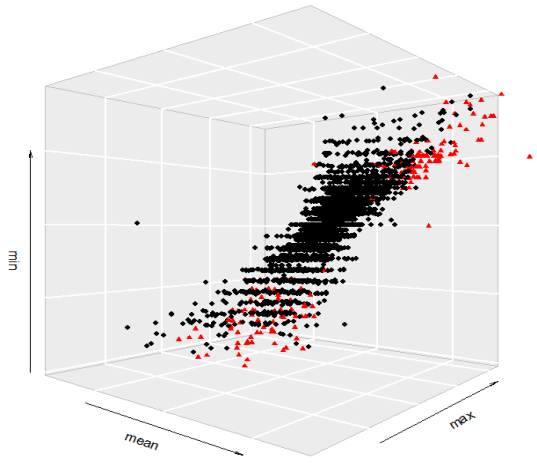

Fig. 4. OC-SVM results using the polynomial kernel function with the hyperparameter values: $D = 3$, $\sigma = 2^{-1}$, $\nu = 0.95$ (•: Normal, ▲: Abnormal).

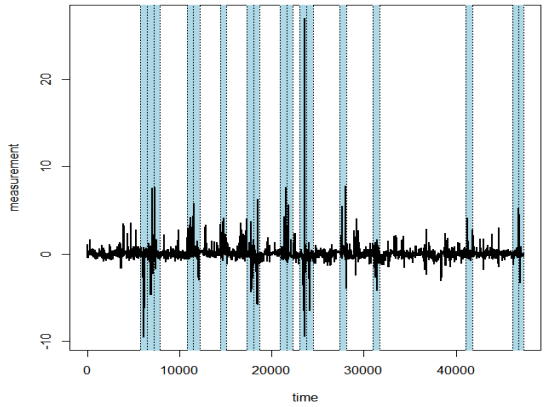

(a) Difference of measurements between sensors 1 and 2

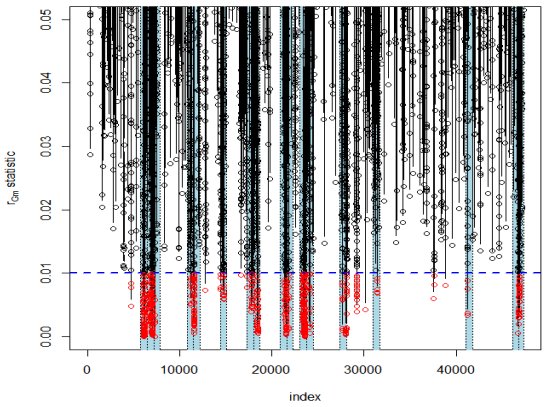

(b) Nonparametric r chart based on Mahalanobis depth

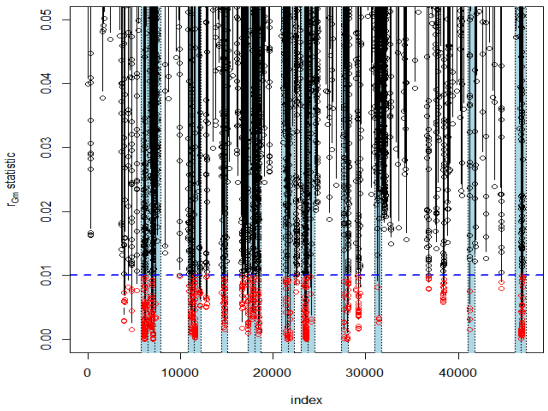

(c) Nonparametric r chart based on Tukey depth

Fig. 5. Application results of nonparametric r chart based on Mahalanobis depth and Tukey depth.

nations of the hyperparameters of OC-SVM can be selected by the grid-search or the random search. The optimal values of the hyperparameters may be determined by using optimization methods, e.g., Bayesian optimization. However, the optimization of the hyperparameter values is out of our research boundary, thus we employed the simple grid-search method.

Table 2 shows the number of intervals containing the outliers corresponding to the hyperparameters in the RBF kernel of the OC-SVM. The results show that the number of intervals including outliers is independent of the hyperparameter values. However, the number of interval estimation including outliers depends on the hyperparameter values when we apply the polynomial kernel function in the OC-SVM. It can be clearly observed in Table 3. Based on the results from the polynomial kernel function, we determined the hyperparameter values corresponding to the 17 intervals as outliers; $D = 3$, $\sigma = 2^{-1}$,

$\nu = 0.95$. The classification results using the OC-SVM with the polynomial kernel function are given in Fig. 4. We select the normally classified data set as reference data set for determining the control limit in control chart adoption procedure.

Next, we conducted the MVN test to select a proper control chart. Table 4 presents the results from Mardia's MVN and Henze-Zirkler's MVN test. At $\alpha = 0.05$ significance level, the reference group does not follow a multivariate normal, and we applied the nonparametric r chart. Fig. 5 shows the application results of r chart. In Fig. 5(a), the intervals classified as faults via OC-SVM are marked with gray-scaled areas. Note that the difference between mean values from two anemometers is greater than 4.1 in those areas. Figs. 5(b) and (c) clearly show that the r charts based on data depths have a strong detect powers of the faults from the anemometer sensors. Note that the OV-SVM and r charts results are closely overlapped with each other.

6. Conclusions

This research proposes a condition monitoring scheme using multivariate control charts based on OC-SVM. The decision function of the OC-SVM is used to define the reference data set in normal condition of the system of interest. We select a suitable multivariate control chart by using the multivariate normality test methods. If the multivariate normality is satisfied, Hotelling's T^2 chart is employed to monitor the health status of the system, otherwise, a nonparametric r chart based on Mahalanobis depth or Tukey depth is applied. The proposed condition monitoring scheme is applied to sensor data of two anemometers to validate our proposed idea. The nonparametric r chart based on the Mahalanobis depth is shown to be more consistent results with OC-SVM.

Recently, Zong et al. [30] proposed a deep autoencoding Gaussian mixture model for unsupervised anomaly detection on high-dimensional data. It provides valuable information about input data in a low-dimensional space, improving the performance of a Gaussian mixture model (GMM) to deal with density estimation tasks. Future research directions include a condition monitoring using deep autoencoding Gaussian mixture model for defining the reference data in phase I of the parametric or nonparametric control chart.

Acknowledgments

This work was supported by the Human Resources Program in Energy Technology of the Korea Institute of Energy Technology Evaluation and Planning (KETEP), granted financial resource from the Ministry of Trade, Industry & Energy, Republic of Korea (No. 20174030201750), and the research fund of Hanyang University (HY-2018, No. 201800000002372).

Nomenclature

$\mathbf{x}$: Train data
$\mathbf{y}$: New observation data
$\mathbf{z}$: Reference data
$\mathbf{w}$: Solution of OC-SVM
m : Number of observations
p : Number of variable
ξ_i : Non-zero slack variable
v : Upper bound on the fraction of outliners
α_i, β_i : Lagrangian multiplier
$k(\cdot)$: Kernel function
$\boldsymbol{\mu}$: Mean vector
Σ : Variance-covariance matrix
$\bar{\mathbf{z}}$: Sample mean vector
$\boldsymbol{S}$: Sample variance-covariance matrix

References

[1] N. H. Kim, D. An and J. H. Choi, *Prognostics and Health Management of Engineering Systems: An Introduction*, Springer (2016).
[2] A. K. S. Jardine, D. Lin and D. Banjevic, A review on machinery diagnostics and prognostics implementing condition-based maintenance, *Mechanical Systems and Signal Processing*, 20 (2006) 1483-1510.
[3] H. Hotelling, Multivariate quality control, *Techniques of Statistical Analysis*, McGraw-Hill, New York (1947).
[4] C. A. Lowry, W. H. Woodall, C. W. Champ and S. E. Rigdon, A multivariate EWMA control charts, *Technometrics*, 34 (1992) 46-53.
[5] W. H. Woodall and M. M. Ncube, Multivariate CUSUM quality control procedures, *Technometrics*, 27 (1985) 285-292.
[6] C. A. Lowry and D. C. Montgomery, A review of multivariate control charts, *IIE Transactions*, 27 (1995) 800-810.
[7] A. J. Hayter and K. L. Tsui, Identification and quantification in multivariate quality control problems, *Journal of Quality Technology*, 26 (1994) 197-208.
[8] R. Sun and F. Tsung, A kernel distance based multivariate control chart using support vector methods, *International Journal of Production Research*, 41 (2003) 2975-2989.
[9] S. J. Bae, G. Do and P. Kvam, On data depth and the application of nonparametric multivariate statistical process control charts, *Applied Stochastic Models in Business and Industry*, 32 (2016) 660-676.
[10] T. Sukchotrat, S. B. Kim and F. Tsung, One-class classification-based control charts for multivariate process monitoring, *IIE Transactions*, 42 (2010) 107-120.
[11] S. He, W. Jiang and H. Deng, A distance-based control chart for monitoring multivariate processes using support vector machines, *Annals of Operations Research*, 263 (2018) 191-207.
[12] H. Rasay, M. S. Fallahnezhad and Y. Zaremehrjerdi, Application of multivariate control charts for condition based maintenance, *International Journal of Engineering*, 31 (2018) 597-604.
[13] S. J. Bae, B. M. Mun, W. Chang and B. Vidakovic, Condition monitoring of a steam turbine generator using wavelet spectrum based control chart, *Reliability Engineering and System Safety*, 184 (2019) 13-20.

[14] V. Vapnik, *Statistical Learning Theory*, Wiley, New York (1998).
[15] A. Karatzoglou, D. Meyer and K. Hornik, Support vector machines in R, *Journal of Statistical Software*, 15 (9) (2006) 1-28.
[16] B. Schölkopf, A. J. Smola, R. C. Williamson and P. L. Bartlett, New support vector algorithms, *Neural Computation*, 12 (2000) 1207-1245.
[17] D. M. J. Tax and R. P. W. Duin, Support vector domain description, *Pattern Recognition Letters*, 20 (1999) 1191-1199.
[18] D. M. J. Tax and R. P. W. Duin, Support vector data description, *Machine Learning*, 54 (2004) 45-66.
[19] B. Schölkopf, J. C. Platt, J. Shawe-Taylor, A. J. Smola and R. C. Williamson, Estimating the support of a high-dimensional distribution, *Neural Computation*, 13 (2001) 1443-1471.
[20] R. L. Mason and J. C. Young, *Multivariate Statistical Process Control with Industrial Applications*, American Statistical Association and Society for Industrial and Applied Mathematics, Philadelphia, PA (2002).
[21] R. Y. Liu, Control charts for multivariate processes, *Journal of the American Statistical Association*, 90 (1995) 1380-1387.
[22] J. W. Tukey, Mathematics and the picturing of data, *Proceedings of the International Congress of Mathematicians*, Vancouver, 2 (1975) 523-531.
[23] Y. Zuo and R. Serfling, General notions of statistical depth function, *Annals of Statistics*, 28 (2000) 461-482.
[24] P. C. Mahalanobis, *On the Generalized Distance in Statistics*, National Institute of Science of India (1936).
[25] F. B. Alt, Multivariate quality control, *The Encyclopedia of Statistical Science*, John Wiley, New York (1984).
[26] J. E. Jackson, Multivariate quality control, *Communications in Statistics - Theory and Methods*, 14 (1985) 2657-2688.
[27] K. V. Mardia, Measures of multivariate skewness and kurtosis with applications, *Biometrika*, 57 (1970) 519-530.
[28] N. Henze and B. Zirkler, A class of invariant consistent tests for multivariate normality, *Communications in Statistics - Theory and Methods*, 19 (1990) 3595-3617.
[29] L. Sun, C. Chen and Q. Cheng, Feature extraction and pattern identification for anemometer condition diagnosis, *International Journal of Prognostics and Health Management*, 3 (2012) 8-18.
[30] B. Zong, Q. Song, M. R. Min, W. Cheng, C. Lumezanu, D. Cho and H. Chen, Deep autoencoding gaussian mixture model for unsupervised anomaly detection, *6th International Conference on Learning Representations* (2018).

Byeong Min Mun received the Ph.D. degree from the Department of Industrial Engineering, Hanyang University, Seoul, Korea. He is a Research Professor in the Department of Industrial Engineering at Hanyang University, Seoul, Korea. His current research interests include reliability, big data, and artificial intelligence.

Munwon Lim is in Ph.D. course in Department of Industrial Engineering, Hanyang University, Seoul, Korea. Her current research interests include signal processing, data mining, prognostics and health management.

Suk Joo Bae received the Ph.D. degree from the School of Industrial and Systems Engineering at the Georgia Institute of Technology, Atlanta, GA, USA, in 2003. He is a Professor in the Department of Industrial Engineering at Hanyang University, Seoul. He published more than 70 papers in journals such as Technometrics, Journal of Quality Technology, IIE Transactions, IEEE Transactions on Reliability, and Reliability Engineering & System Safety.